Total cross sections of electron-impact ionization of Ar^{7+}

Y. Zhang, C. B. Reddy, R. S. Smith, D. E. Golden, and D. W. Mueller
Department of Physics, University of North Texas, Denton, Texas 76203-5368

D. C. Gregory
Physics Division, Oak Ridge National Laboratory, Oak Ridge, Tennessee 37831-6372
(Received 16 September 1991)

The electron-impact single-ionization cross section of Ar^{7+} has been measured from 18 to 1186 eV using a crossed-beams technique. The present results are higher than previous measurements at the higher energies and are in good agreement with recent distorted-wave calculations that include contributions from excitation autoionization. Below the threshold for direct ionization at 144 eV, the cross section contains contributions due to space-charge modulation and excitation of metastable ions in the target beam into autoionizing states. These transitions are predominantly spin allowed and dipole forbidden. Scaling laws for sodiumlike ions are discussed.

PACS number(s): 34.80.Kw, 32.80.Dz

I. INTRODUCTION

Electron-impact ionization of atomic ions is very important in plasma discharges, and these processes have been studied using different techniques. Some systematic cross-section investigations of isonuclear sequences have been made to test scaling laws [1,2]. The Na-like isoelectronic sequence is of particular interest because of its simple outer-shell configuration. The ionization of these ions usually includes excitation-autoionization processes associated with inner-shell excitation since these excited states usually lie above the ionization potential for the less tightly bound valence electrons. In early measurements of Mg^+ [3,4], Al^{2+}, and Si^{3+} [4], discrepancies with calculations due to excitation-autoionization contributions to the cross section were found. Experimental studies using highly charged ions, however, were not feasible until the development of electron-cyclotron-resonance (ECR) ion sources. Measurements of electron-impact ionization of Ar^{7+} of Defrance *et al.* [5] were compared with distorted-wave calculations [2] and indicated significant contributions from excitation-autoionization processes. Recent high energy-resolution measurements on Mg^+ were able to resolve a number of resonant-excitation-double-autoionization (REDA) features [6]. Many of these features were confirmed by an R-matrix calculation including the ground and autoionizing states in the close-coupling expansion [7].

Several authors have used *ab initio* calculations to evaluate the contributions to the cross sections from direct and indirect ionization processes [2,8–10]. Early work of Bely on Mg^+ using a Coulomb-Born approximation overestimated the excitation-autoionization contribution presumably because stabilization by radiative decay from the intermediate excited states was neglected [8]. Later experimental work by Martin *et al.* did not agree with this calculation [3]. Distorted-wave calculations by Younger give the cross section and the rate coefficients for direct ionization from ground-state Ar^{7+} [2]. Distorted-wave calculations which include excitation and autoionization branching ratios have been made for the sodiumlike isoelectronic ions Mg^+, Al^{2+}, Si^{3+} [9] and Ti^{11+}, Cr^{13+}, Fe^{15+}, Ni^{17+} [10]. The total ionization cross section was taken as the sum of the direct and indirect contributions using a statistically averaged population of upper excited states and using branching ratios calculated individually for the different excited configurations. This approach [10] gave better agreement with experiments [11,12] for several ion species. Close-coupling calculations on Mg^+, Al^{2+}, and Si^{3+} by Henry and Msezane [13] which took REDA into account resolved some of the discrepancies between the experimental results [4] and the distorted-wave calculations [9].

The present work focuses on crossed-beam measurements of electron-impact ionization of Ar^{7+} in the energy range of 18 to 1186 eV. In this energy domain two interesting processes are present: ionization contributions from metastable excited states which lie above the direct ionization threshold and excitation autoionization from the ground state.

II. THE ATOMIC PROCESSES CONSIDERED

Relativistic Hartree-Fock calculations of the energy levels of Ar^{7+} and Ar^{8+} are shown in Fig. 1 [14]. The processes labeled 1, 2, and 3 depict direct knockout of a $3s$, a $2p$, and a $2s$ electron, respectively, from the Ar^{7+} ground state ($2p^6 3s$). The many excited configurations of $Ar^{7+}(2p^6 nl)$ are not shown individually. They usually decay through radiative transitions with lifetimes $\tau < 10^{-8}$ s and have therefore decayed by the time the ions reach the interaction chamber. The lowest inner-shell excited states ($2p^5 3s^2$ manifold) lie above the energy of the ground state of the daughter Ar^{8+} ion ($2p^6$). Most of the inner-shell excited states autoionize rapidly (10^{-10} s) although some of the quartet states are metastable [15]. For Ar^{7+}, the quartet $2p^5 3s 3p$ ions are estimated to have $\tau > 10^{-6}$ s [16]. Metastable ions that spontaneously au-

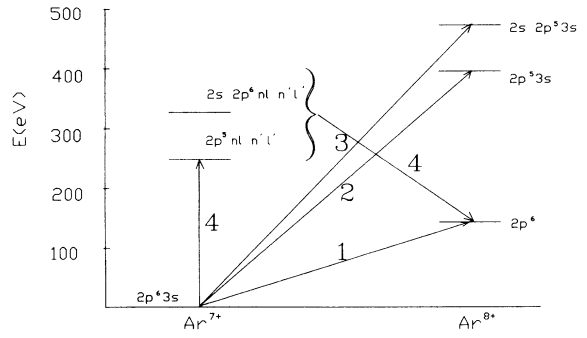

FIG. 1. Energy-level diagrams of Ar^{7+} and Ar^{8+} and the ionization channels considered. 1, direct knockout of a $3s$ electron; 2, direct knockout of a $2p$ electron; 3, direct knockout of a $2s$ electron; 4, excitation autoionization of a ground state Ar^{7+}.

toionize in the interaction chamber would be expected to make a large contribution to the experimental background ion signal [17]. Electron collisions with the remaining metastables can excite quartet metastable ions to the neighboring autoionizing states. This process would contribute to the electron-impact ionization signal and be observed in the energy region below the threshold for direct ionization. Because the threshold energy for this excitation is small (~ 1 eV), the contribution to the signal is expected to be in the high-energy asymptotic limit when the incident energy in the experiment is near the threshold for direct ionization of the ground state.

In the energy region just above the direct-ionization threshold (144 eV), direct ionization is expected to be the major ionization process. Above the threshold for excitation from the ground state to $2p^5 3snl$ (about 250 eV), excitation autoionization is expected to make significant contributions to the ionization cross section.

III. EXPERIMENT

A complete description of the apparatus has been given previously [18] and only a brief description of the apparatus is given here. The Ar^{7+} ions generated in the electron-cyclotron-resonance ion source [19] are extracted, accelerated to 70 keV, and mass-selected before entering the interaction region. For this work, the beam current was about 30 nA. A magnetically confined electron beam crosses the ion beam at 90° [20,21] with an estimated energy spread of about 2 eV or less [18,22]. After passing through the interaction region, the ion beam is separated magnetically into different charge states by a magnetic sector. The Ar^{8+} ions are counted using a channeltron detector. Movable slits are used to measure the profiles of the ion and the electron beams to determine the scattering form factor F [23]. The form factor is a measure of overlap of the ion and electron beams. The primary ion and electron currents are collected in Faraday cups and time integrated. The cross sections are determined using the relationship

$$\sigma(E)=\frac{R(E)}{I_e I_i}\frac{qe^2 v_e v_i}{(v_e^2+v_i^2)^{1/2}}\frac{F}{D}, \tag{1}$$

TABLE I. Cross-section uncertainties. All uncertainties are listed at equivalence to one standard deviation in statistics.

Source	Uncertainty (%)
Statistical uncertainty	8
Form factor	3
Systematic uncertainties	
Particle counting efficiency	5
Transmission to signal ion detector	5
Ion current	3
Electron current	1
Space-charge modulation and excitation autoionization of metastable ions	16
Combined: Total uncertainty at the peak of cross section	20

where $\sigma(E)$ is the ionization cross section; q is the charge number of the parent ion; F is the form factor; I_e and I_i are the electron and ion currents, respectively; v_e and v_i are the velocities of the electrons and ions, respectively; D is the ion detection efficiency; and $R(E)$ is the ionization count rate [23]. Since the background signal is generally larger than the electron-impact-ionization signal, the electron beam is modulated and the difference between the signal with the electron beam on and that with the electron beam off is used to measure the signal due to electron collisions. Consistency checks were made during the experiment by repeating measurements of the ionization cross sections at 75, 100, and 600 eV to ensure that the experimental conditions did not change as a function of time.

The experimental uncertainties are listed in Table I. Statistical and other measurement errors have been determined as in previous measurements [18,24]. The estimated errors for space-charge modulation and excitation autoionization of metastable ions are discussed in Sec. IV.

IV. RESULTS AND DISCUSSIONS

A. Below-threshold behaviors

The raw ionization cross-section data below the direct-ionization threshold from the ground state of Ar^{7+} (144 eV) are shown in Fig. 2 (crosses). Below threshold, we measured a signal that increased with decreasing electron energy. This is presumed to be due to a combination of electron space charge and excitation autoionization of some metastable ions.

Electron space-charge effects can cause the background count rate to change. This effect is proportional to the charge density of the electron beam which gives the cross section an energy dependence of

$$\sigma_{\text{sp ch}}=\frac{A}{\sqrt{E}}, \tag{2}$$

where A is a constant dependent on experimental conditions [25].

Another contribution to the cross section below the ground-state threshold for direct ionization is due to excitation of metastables to autoionizing states. The lowest

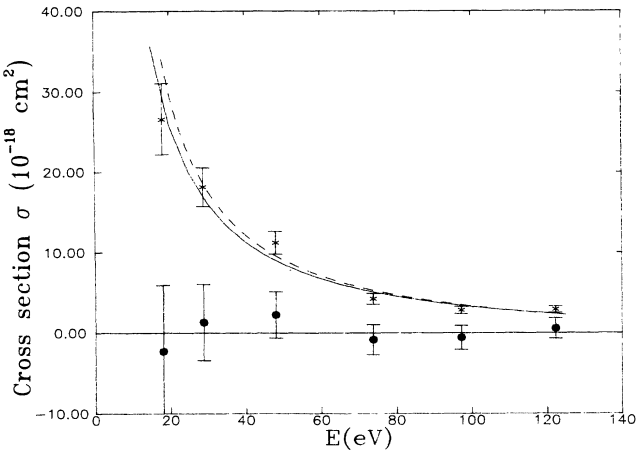

FIG. 2. Cross sections below the direct-ionization threshold. Crosses, measured (raw) data; closed circles, data after the correction for space-charge modulation and excitation autoionization of metastable ions (subtracting the fitting of trial 5 in Table II); dashed line, least-squares-ftting result, represented by Eq. (6) with trial 4 in Table II; solid line, least-squares-fitting result, represented by Eq. (6) with trial 5 in Table II.

electron energy used in our experiment, 18 eV, is much larger than the energies for excitation of the metastable ions to these states (estimated to be 1 to 2 eV); thus, we have used the asymptotic forms for the excitation cross sections to approximate these contributions in the present measurements [26,27]. Three excitation processes are considered for Ar^{7+}: (a) spin-allowed, dipole-allowed excitation:

$$\sigma_{SA}(E)=B\frac{\ln(4E/E_{if})}{E}=B\frac{\ln(E)}{E}-B\frac{\ln(E_{if}/4)}{E}\ , \tag{3}$$

where B is a constant to be determined and E_{if} is the excitation energy; (b) spin-allowed, dipole-forbidden excitation:

$$\sigma_{DF}(E)=\frac{C'}{E}\ ; \tag{4}$$

and (c) spin-forbidden excitation:

$$\sigma_{SF}(E)=\frac{D}{E^3}\ . \tag{5}$$

Combining space-charge modulation with processes (a), (b), and (c), the excitation cross section has the following form:

$$\sigma=\frac{A}{\sqrt{E}}+\frac{B\ln(E)}{E}+\frac{C}{E}+\frac{D}{E^3}\ , \tag{6}$$

where A, B, C, and D are parameters to be determined by fitting the data below threshold. The first term will be nonzero if space-charge modulation is present. The second and third terms are tied to process (a) since the parameter C is equal to $C'-B\ln(E_{if}/4)$. The third term is connected to process (b). The fourth term will be nonzero if process (c) contributes to the cross section.

The data below threshold were fit with Eq. (6) using a least-squares criterion [28] with the following restrictions: coefficients B and D were required to be positive because processes (a) and (c) can only add to the measured cross section. The coefficients for some possible fits are given in Table II. The first three fits have negative values of B and are discarded. The last five trials give large χ^2's and are discarded. Fitting trial 6 gives a negative B and hence is also discarded. Fitting trials 4 and 5 give the best physically plausible fits, and yield the same results within the uncertainties of the coefficients. The fact that coefficient A is negative indicates that the electron space charge results in a loss of signal. The curves resulting from trials 4 and 5 have been plotted in Fig. 2 (dashed line and solid line, respectively). The presence of the $(1/E)$ term ($C\neq 0$) indicates that excitation of metastable ions is primarily due to spin-allowed, optically forbidden transitions. Since the error for D is more than three times the value of D in trial 4, we cannot say whether or not spin-forbidden excitation is present.

The measured and corrected cross sections are tabulated in Table III together with their estimated uncertainties. The cross sections have been corrected for space charge and excitation autoionizations from metastable ions by subtracting Eq. (6) with coefficients determined in trial 5 in Table II. The uncertainties have been estimated

TABLE II. Least-squares fitting of the coefficients (blanks indicate that the coefficient is not included in the fitting).

Trial number	A	B	C	D	χ^2
1	3.7±2.0[2][a]	−1.9±0.9[3]	5.3±2.2[3]	−3.1±1.5[4]	3.6
2		−2.0±0.9[2]	1.2±0.4[3]	−5.6±6.1[4]	7.0
3	−0.7±8.0[1]	−1.0±3.0[2]	8.6±5.7[2]		7.8
4	−4.0±1.9[1]		7.3±1.9[1]	1.7±4.9[4]	7.8
5	−3.5±1.0[1]		6.7±0.9[2]		7.9
6		−1.3±0.3[2]	9.2±1.6[2]		7.8
7	3.3±0.3[1]			1.5±0.2[5]	23.3
8			3.4±0.3[2]	7.0±2.7[4]	12.3
9	3.9±0.3[1]				61.0
10			3.7±0.2[2]		19.0
11				2.5±0.2[5]	174.5

[a]Numbers enclosed in square brackets indicate multiplicative powers of ten.

from

$$(\delta\sigma)^2=(\delta\sigma_{\text{measured}})^2+\left[\frac{\delta A}{\sqrt{E}}\right]^2+\frac{1}{4}\left[\frac{A}{E^{3/2}}\right]^2(\delta E)^2 + \left[\frac{\delta C}{E}\right]^2+\left[\frac{C}{E^2}\right]^2(\delta E)^2 . \quad (7)$$

B. Above-threshold behaviors

The corrected data are plotted in Fig. 3 and compared with the previous results of Defrance *et al.* [5] and calculated predictions [2,29,30]. For energies below about 300 eV, the agreement between the present and the previous results is good. However, at energies above 350 eV, the present results are larger than the results of Defrance *et al.* [5]. The solid line in Fig. 3 is the distorted-wave calculation of Griffin *et al.* for the direct ionization of $3s$ electron knockout plus the excitation autoionization with an assumed branching ratio of 1 [29]. The short dashed line only includes the direct knockout of a $3s$ electron [29]. The data show evidence of indirect processes in the energy range from 150 to 500 eV and are in good agreement with the calculations of Griffin *et al.* [29]. At higher energies ($E > 500$ eV), the cross sections are higher than the calculations, possibly due to direct ionization from the $2p$ and $3s$ states. The very short dashed line on the figure is given by the semiempirical formula of Lotz [30] for direct ionization from the ground state (direct knockout of one $3s$, $2p$, or $2s$ electron; processes 1, 2, and 3 in Fig. 1). The long dashed line is from a fit of the direct-ionization cross section for the Na-like isoelectronic sequence based on distorted-wave calculations [2]. The present data give a cross section that is larger than either of these predictions for $E > 350$ eV, probability due to excitation autoionization from the ground state.

TABLE III. Ionization cross sections.

Electron energy E (eV)	Ionization cross sections σ (10^{-18} cm^2) Measured data	Corrected data[a]
18.1	26.63±4.34	−2.29±8.21
28.8	18.15±2.41	1.30±4.73
48.0	11.24±1.41	2.25±2.87
73.8	4.23±0.67	−0.83±1.88
97.2	0.81±0.44	−0.58±1.49
122.3	2.91±0.40	0.56±1.27
170.2	3.11±0.69	1.82±1.18
195.0	1.83±0.14	0.87±0.89
243.0	1.56±0.21	1.02±0.80
267.1	1.76±0.26	1.37±0.77
291.8	1.83±0.29	1.56±0.75
364.3	3.19±0.23	3.16±0.64
390.0	3.28±0.29	3.31±0.65
413.0	3.45±0.20	3.53±0.59
440.0	2.99±0.26	3.12±0.60
489.0	3.21±0.24	3.40±0.56
538.0	3.09±0.36	3.33±0.60
561.0	3.51±0.22	3.78±0.52
586.9	3.04±0.08	3.32±0.46
593.6	2.91±0.13	3.20±0.47
643.5	2.77±0.23	3.10±0.49
692.7	2.88±0.18	3.22±0.45
742.3	2.76±0.17	3.13±0.43
792.1	2.94±0.16	3.32±0.42
840.0	3.07±0.27	3.46±0.46
890.0	2.85±0.23	3.25±0.43
988.0	2.56±0.23	2.99±0.41
1087.0	2.31±0.22	2.75±0.39
1186.0	2.20±0.22	2.64±0.38

[a]The data have been corrected for space charge and excitation autoionization from metastable ions, by subtracting Eq. (6) with coefficients determined in trial 5 in Table II.

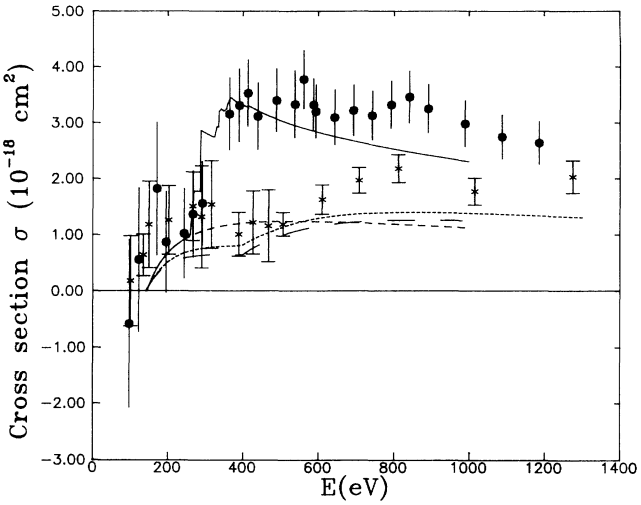

FIG. 3. Cross sections near and above the direct-ionization threshold. Closed circles, present measurement with corrections for space-charge modulation and metastable ions; crosses, measurements of Defrance *et al.*, Ref. [5]. Solid line, distorted-wave calculations by Griffin *et al.*, Ref. [29] including excitation autoionization from the ground state, short dashed line, distorted-wave calculation with only direct ionization of a $3s$ electron, Ref. [29]; very short dashed line, prediction by the Lotz formula, Ref. [30]; long dashed line, fitted formula for the Na-isoelectronic sequence by Younger, Ref. [2].

C. Comparisons with other Na-like ions

The Na-like isoelectronic sequence has been studied extensively. In this section we will compare the relative contributions to the cross section from indirect and direct ionization for the present Ar^{7+} data and previous measurements for Mg^{+}, Al^{2+}, Si^{3+} [4], Ti^{11+}, Cr^{13+} [12], and Fe^{15+} [11]. Calculations [8] showed that the contribution of excitation autoionization increases with increasing charge number. Similar behavior was found for the siliconlike ions in the scaling of ionization cross sections of Cr^{10+} and Ni^{14+} [31]. However, for sodiumlike ions with charge state $11 < q < 17$, the autoionization branching ratio decreases with increasing charge state and the resulting ratio of excitation autoionization to direct ionization is almost constant [10]. We have tabulated the ratio of the total ionization cross section to the direct ionization predicted by the calculations of Younger [2] in

TABLE IV. Ratios of total-ionization cross sections (σ_T) to the direct-ionization cross sections (σ_D) of Na-like ions. The direct-ionization cross sections (σ_D) are the results of the scaling of the distorted-wave calculations by Younger (Ref. [2]). The theoretical ratios are listed at energies where the distorted-wave calculations predict the maximum contributions of the indirect ionization. The experimental measurements are listed at energies closest to the energies provided by the theoretical prediction.

Ion	E (eV)	σ_T/σ_D(theor)	σ_T(expt)/σ_D(theor)
Mg^+	64[a]	1.3[b]	0.90±0.08[a]
Al^{2+}	95[a]	2.0[b]	0.87±0.07[a]
Si^{3+}	139[a]	2.1[b]	1.6±0.2[a]
Ar^{7+}	364[c]	5.4[d]	5.3±0.4[c]
Ti^{11+}	688[e]	5.4[f]	4.6±0.2[e]
Cr^{3+}	885[e]	4.9[f]	5.0±0.5[e]
Fe^{15+}	988[g]	5.0[f]	5.8±0.9[g]

[a]Crandall *et al.*, Ref. [4].
[b]Griffin *et al.*, Ref. [9].
[c]This work.
[d]Griffin *et al.*, Ref. [29].
[e]Gregory *et al.*, Ref. [12].
[f]Griffin *et al.*, Ref. [10].
[g]Gregory *et al.*, Ref. [11]. The ratio was taken at the maximum energy of the experimental measurements of 988 eV, while the theory[f] predicts the maximum contribution of indirect ionization is given at $E = 1100$ eV.

Table IV. The ratios are given at electron energies where the calculations by Griffin *et al.* [9,10,29] predict the maximum contribution from indirect ionization. In the case of Fe^{15+}, we used 988 eV, which is the largest energy at which experimental data are available [11]. For the lighter ions, the distorted-wave calculations of Younger [2] seem to overestimate the direct-ionization contribution. This is evidenced by the ratios σ_T(expt)/σ_D(theor) being less than 1 for Mg^+ and Al^{2+}. Our Ar^{7+} result is in agreement with the calculation [29] which assumed a branching ratio of 1 for autoionization. The resulting ratio ($\sigma_T/\sigma_D \approx 5$) is close to that given for ions with higher charge numbers. It would be interesting to measure σ_T for other ions in the Na-like electronic sequence (especially for P^{4+}, S^{5+}, Cl^{6+}, K^{8+}, Ca^{9+}, and Sc^{10+}) and compare these ratios with the results accumulated thus far.

V. CONCLUSIONS

In this investigation, the electron-impact single-ionization cross section of Ar^{7+} has been measured from about 18 to 1186 eV. For energies below the direct-single-ionization threshold, the data show space-charge modulation and excitation autoionization from metastable ions, dominated by spin-allowed, dipole-forbidden transitions. At energies above the direct-ionization threshold, the present results indicate a larger contribution from excitation autoionization than the previous results of Defrance *et al.* [5] and are in good agreement with the distorted-wave calculations of Griffin *et al.* over the entire energy range [29]. The present measurements give a ratio of indirect-to-direct-ionization cross-section contributions in good agreement with the previous Ti^{11+}, Cr^{13+}, and Fe^{15+} measurements and calculations [11,12,10].

ACKNOWLEDGMENTS

We wish to thank R. A. Phaneuf, D. C. Griffin, M. S. Pindzola, and C. Bottcher for valuable discussions. We thank J. W. Hale for his technical assistance. This work was supported by the Office of Fusion Energy, U.S. Department of Energy, under Contract No. DE-AC05-84-OR21400 with Martin Marietta Energy Systems, Inc. Travel support was provided for the University of North Texas collaborators by the National Science Foundation under Grant No. PHY-88-03562.

[1] S. M. Younger, Phys. Rev. A **23**, 1138 (1981).
[2] S. M. Younger, Phys. Rev. A **24**, 1272 (1981).
[3] S. O. Martin, B. Peart, and K. T. Dolder, J. Phys. B **1**, 537 (1968).
[4] D. H. Crandall, R. A. Phaneuf, R. A. Falk, D. S. Belic, and G. H. Dunn, Phys. Rev. A **25**, 143 (1982).
[5] P. DeFrance, J. Phys. (Paris) Colloq. (Suppl.) **50**, C1-299, (1989); Proceedings of the International Conference on the Physics of Multiply Charged Ions and International Workshop on E.C.R. Ion Sources, Grenoble, France, 1988 (unpublished).
[6] A. Müller, G. Hoffman, K. Tinschert, B. Weissbecker, and E. Salzborn, Z. Phys. D **15**, 145 (1990).
[7] S. S. Tayal, J. Phys. B **24**, L219 (1991).
[8] O. Bely, J. Phys. B **1**, 23 (1968).
[9] D. C. Griffin, C. Bottcher, and M. S. Pindzola, Phys. Rev. A **25**, 154 (1982).
[10] D. C. Griffin, M. S. Pindzola, and C. Bottcher, Phys. Rev. A **36**, 3642 (1987).
[11] D. C. Gregory, L. J. Wang, F. W. Meyer, and K. Rinn,

Phys. Rev. A **35**, 3256 (1987).
[12] D. C. Gregory, L. J. Wang, D. R. Swenson, M. Sataka, and S. J. Chantrenne, Phys. Rev. A **41**, 6512 (1990).
[13] R. J. W. Henry, and A. Z. Msezane, Phys. Rev. A **26**, 2545 (1982).
[14] R. D. Cowan, *The Theory of Atomic Structure and Spectra* (California Press, Berkeley, CA, 1981).
[15] S. E. Harris, D. J. Walker, R. G. Caro, A. J. Mendelson, and R. D. Cowan, Opt. Lett. **9**, 168 (1984).
[16] D. C. Gregory and R. A. Phaneuf (private communication).
[17] A. M. Howald, D. C. Gregory, F. W. Meyer, R. A. Phaneuf, A. Müller, N. Djuric, and G. H. Dunn, Phys. Rev. A **33**, 3779 (1986).
[18] D. C. Gregory, F. W. Meyer, A. Müller, and P. Defrance, Phys. Rev. A **34**, 1757 (1986).
[19] F. W. Meyer, Nucl. Instrum. Methods Phys. Res. B **9**, 532 (1985).
[20] P. O. Tayler, K. T. Dolder, W. E. Kauppila, and G. H. Dunn, Rev. Sci. Instrum. **45**, 538 (1974).
[21] P. O. Tayler, Ph.D. dissertation, University of Colorado, 1974.
[22] D. S. Belic, R. A. Falk, G. H. Dunn, D. C. Gregory, C. Cisneros, and D. H. Crandall, Bull. Am. Phys. Soc. **26**, 1315 (1981).
[23] E. Salzborn, in *Physics of Ion-Ion and Electron-Ion Collisions,* Vol. 83 of *NATO Advanced Study Institute, Series B: Physics,* edited by F. Brouillard and J. W. McCowan, (Plenum, New York, 1983), pp. 239–277.
[24] Y. Zhang, C. R. Reddy, R. S. Smith, D. E. Golden, D. W. Mueller, and D. C. Gregory, Phys. Rev. A **44**, 4368 (1991).
[25] M. F. A. Harrison, Br. J. Appl. Phys. **17**, 371 (1966).
[26] R. J. W. Henry, Phys. Rep. **68**, 1 (1981).
[27] D. H. Crandall, in *Atomic Physics of Highly Ionized Atoms,* Vol. 96 of *NATO Advanced Study Institute, Series B: Physics,* edited by R. Marrus (Plenum, New York, 1983), pp. 399–453.
[28] J. Mathews and R. L. Walker, *Mathematical Methods of Physics,* 2nd ed. (Benjamin, New York, 1970).
[29] D. C. Griffin, C. Bottcher, and M. S. Pindzola (private communication).
[30] W. Lotz, Z. Phys. **206**, 105 (1967); **216**, 241 (1968); **220**, 466 (1969).
[31] M. Sataka, S. Ohtani, D. Swenson, and D. C. Gregory, Phys. Rev. A **39**, 2397 (1990).